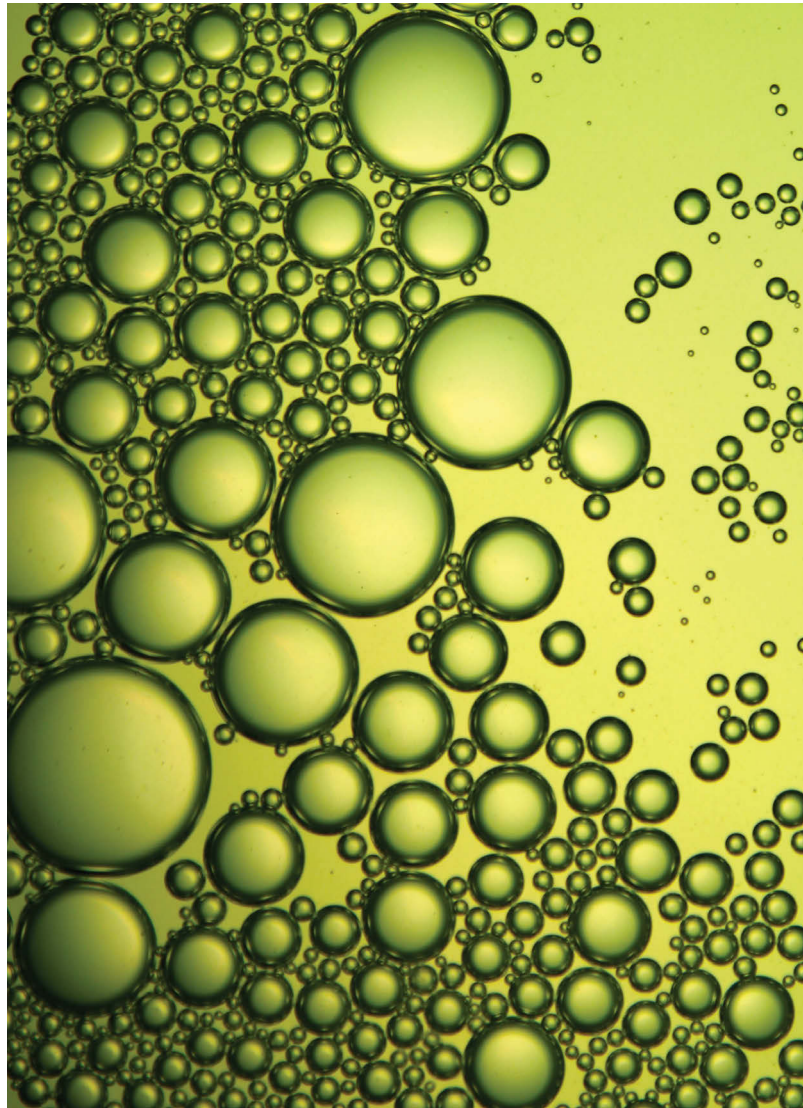


# ENHANCING BIOFUEL PRODUCTION FROM A MARINE MICROALGAE- CONSTRAINTS OF CULTIVATION SCALE-UP



**Dale T. Radford**

B.Sc (Hons), MRes

Submitted in fulfillment of the requirements for the degree of Doctor of Philosophy in  
Science,

Climate Change Cluster (C3),  
School of Life Sciences,

University of Technology Sydney,

May 2016

## **Certificate of Original Authorship**

---

I certify that the work in this thesis has not previously been submitted for a degree nor has it been submitted as part of requirements for a degree except as fully acknowledged within the text.

I also certify that the thesis has been written by me. Any quotations, ideas and help that I have received in my research work and during the preparation of the thesis itself have been acknowledged. In addition, I certify that all information sources and literature used are indicated in the thesis.

Signed: \_\_\_\_\_

Dale Radford (PhD candidate)

## **Acknowledgements**

---

Thank you to my supervisors, Peter Ralph, John Raven, Milán Szabó and Martin Schliep for their support, guidance and critique throughout my candidature. Thank you to all members of the Algal Biosystems Group at UTS who have provided continued support both in technical and intellectual challenges that have allowed for the completion of this thesis. To my fellow PhD students, Kirralee Baker, Charlotte Robinson and Michaela Larsson, for their assistance overcoming laboratory challenges whilst also reminding me of the world outside of university and the beautiful country that is Australia. And, finally to the friendly faces at Knights Tea & Coffee Company for fulfilling my caffeine addiction over the past 3 years.

## Preface

---

This thesis has been prepared in publication format, whereby each chapter represents a manuscript ready for submission to a peer-reviewed journal. As of yet, no individual chapter has been accepted for publication in a peer-reviewed journal.

In association with my PhD, I have been co-author on two publications that are relevant to the thesis, but does not contribute to it. The work presented in Tamburic et al .2014 lead up to the work presented in **Chapter 2**. The concepts and methods underlying Baker et al. 2016 provide the foundations for the work presented in **Chapter 3**.

Tamburic, B., Guruprasad, S., **Radford, D.T.**, Szabó, M., Lilley, R.M., Larkum, A.W.D., Franklin, J.B., Kramer, D.M., Blackburn, S.I., Raven, J. A, Schliep, M. & Ralph, P.J. 2014. The Effect of Diel Temperature and Light Cycles on the Growth of *Nannochloropsis oculata* in a Photobioreactor Matrix. *PloS one*, 9, 1, p. e86047.

Baker, K.G., Robinson, C.M., **Radford, D.T.**, McInnes, A.S., Evenhuis, C. and Doblin, M.A., 2016. Thermal performance curves of functional traits aid understanding of thermally induced changes in diatom-mediated biogeochemical fluxes. *Frontiers in Marine Science*, 3, p.44.

## Table of Contents

<b>Certificate of Original Authorship .....</b>	<b>ii</b>
<b>Acknowledgements .....</b>	<b>iii</b>
<b>Preface.....</b>	<b>iv</b>
<b>Table of Contents.....</b>	<b>v</b>
<b>List of Figures .....</b>	<b>ix</b>
<b>List of Tables .....</b>	<b>xiv</b>
<b>Supplementary Figures .....</b>	<b>xv</b>
<b>Supplementary Tables.....</b>	<b>xv</b>
<b>Abstract.....</b>	<b>xvi</b>
<b>Chapter 1    General Introduction .....</b>	<b>1</b>
1.1.          Global Energy Challenge .....	1
1.2.          Biofuels .....	2
1.3.          Algal biofuels .....	3
1.3.1.    Overview .....	3
1.3.2.    Energy balance .....	4
1.4.          The microalgae biofuel production process .....	7
1.4.1.    Microalgal cultivation.....	7
1.4.2.    Downstream processing .....	8
1.5.          Constraints in large-scale microalgae cultivations .....	10
1.5.1.    Scale .....	10
1.5.2.    Reactor design and mode of operation constraints .....	10
1.5.3.    Algal strain selection .....	11
1.5.4.    External abiotic environmental factors .....	12
1.5.5.    Nutrient supply .....	15
1.5.6.    Carbon supply .....	16
1.6.          Summary .....	17
1.7.          Thesis outline.....	17
1.8.          General references .....	19

<b>Chapter 2</b>	<b>Laboratory to large-scale: A multi-trait comparison of <i>Nannochloropsis oculata</i> cultivated under static and dynamic environmental conditions. ....</b>	<b>25</b>
2.1	Introduction .....	26
2.2	Materials and Methods .....	29
2.2.1	Microalgal Cultures and medium .....	29
2.2.2	Photobioreactor set-up.....	29
2.2.3	Growth measurements.....	30
2.2.4	Fluorescence measurements.....	31
2.2.5	Nutrient analysis .....	31
2.2.6	Sampling regimes .....	32
2.2.7	Statistical analysis.....	32
2.3	Results.....	33
2.3.1	Growth of <i>N. oculata</i> at different light and temperature regimes .....	33
2.3.2	Nutrient limitation in simulated environmental growth.....	34
2.3.3	Relative photosynthetic electron transport rate.....	38
2.4	Discussion .....	40
2.5	Acknowledgments.....	45
2.6	References .....	45
2.7	Supplementary Figures.....	49
<b>Chapter 3</b>	<b>Time-resolved thermal response of <i>Nannochloropsis oculata</i> improves large-scale cultivation reliability. ....</b>	<b>51</b>
3.1	Introduction .....	52
3.2	Materials and methods .....	55
3.2.1	Stock microalgal culture and medium .....	55
3.2.2	In vivo chlorophyll fluorescence .....	55
3.2.3	Short-term (5 min) temperature stress analysis- MC-PAM .....	56
3.2.4	Long-term (4 day) temperature stress analysis .....	56
3.2.5	Statistical analysis.....	57
3.3	Results.....	58
3.3.1	Short-term thermal response on photophysiology of <i>N. oculata</i> .....	58
3.3.2	Thermal response following 24 hours exposure .....	59
3.3.3	Long-term thermal response .....	61

3.4	Discussion .....	64
3.5	Acknowledgements.....	68
3.6	References .....	68
3.7	Supplementary figures.....	72
<b>Chapter 4</b>	<b>Satisfying the nutrient tank of <i>Nannochloropsis oculata</i> .</b>	<b>74</b>
4.1	Introduction .....	75
4.2	Materials and methods .....	78
4.2.1	Microalgal culture and medium .....	78
4.2.2	Experimental nutrient matrix .....	78
4.2.3	Growth analysis .....	79
4.2.4	Nutrient analysis .....	80
4.2.5	Photophysiological analysis .....	80
4.2.6	Lipid content and fatty acid composition analysis .....	80
4.2.7	Statistical analysis.....	81
4.3	Results and discussion .....	82
4.3.1	Growth and nutrient uptake dynamics .....	82
4.3.2	Physiological dynamics:.....	85
4.3.3	Biochemical response .....	87
4.3.4	Implications to large-scale .....	91
4.3.5	Future directions .....	91
4.4	Acknowledgments.....	93
4.5	References .....	93
4.6	Supplementary Figures.....	97
<b>Chapter 5</b>	<b>Assessing gas transfer rates as an essential link in scale-up studies for mass microalgal cultivation .....</b>	<b>98</b>
5.1	Introduction .....	99
5.2	Materials and methods .....	104
5.2.1	ePBR gas transfer characterisation set-up .....	104
5.2.2	Microalgal culture and medium .....	105
5.2.3	Static cultivation (tank reactor) setup .....	105
5.2.4	Simulated outdoor condition (ePBR) setup .....	105
5.2.5	Growth measurements.....	106
5.2.6	In situ photosynthesis, respiration rate and gas transfer calculations.....	106

5.2.7	Modeling gas-transfer rates, photosynthesis and respiration .....	108
5.3	Results .....	110
5.3.1	Gas transfer characterisation .....	110
5.3.2	Response to static growth conditions .....	112
5.3.3	Response to simulated outdoor growth conditions .....	112
5.4	Discussion .....	116
5.5	Acknowledgements .....	120
5.6	References .....	120
5.7	Supplementary Figures .....	125
<b>Chapter 6</b>	<b>General Discussion .....</b>	<b>127</b>
6.1	The ePBR platform - a suitable technique for improving large-scale biofuel production .....	127
6.2	New insights gained from an in-depth physiological characterisation of a biofuel candidate microalga. I. Understanding constraints on large-scale production. 129	
6.3	New insights gained from an in-depth physiological characterisation of a biofuel candidate microalga. II. Harnessing the natural capacity of microalgae..	131
6.4	Perspectives for future research .....	133
6.5	The future of microalgae biofuel production- concluding remarks ....	135
6.6	General References .....	137



## List of Figures

<b>Figure 1.1</b> Biofuel classification modified from Nigam & Singh (2011).....	2
<b>Figure 1.2</b> A schematic representation of photosynthetic biofuel production (adapted from Schenk et al. 2008). Legend in top left explains arrows. Abbreviations; LHC, light harvesting complex; PSI/II, photosystem I/II; PQ, plastoquinone; PQH <sub>2</sub> , reduced plastoquinone; Cyt b6f; Cytochrome b6/f complex; PC, plastocyanin; Fd, ferredoxin; FNR, ferredoxin/NADPH oxidoreductase; NADPH, reduced nicotinamide adenine dinucleotide phosphate; ADP, adenosine diphosphate; ATP, adenosine triphosphate; P <sub>i</sub> , inorganic phosphate; TAG, triacylglycerol. Underlined products are used in biofuel production.....	6
<b>Figure 1.3</b> Microalgal production process (modified from Pragya et al. 2013), where italics indicate possible downstream processes.....	7
<b>Figure 1.4</b> Reactor design schematic- (a) an aerial view of and open raceway pond; (b) a tubular closed photobioreactor (PBR) with parallel horizontal tube (both taken from Chisti 2007). .....	8
<b>Figure 1.5</b> A typical photosynthesis vs. irradiance (light intensity) curve: A typical photosynthesis response curve where; shaded area is dark respiration, P <sub>max</sub> is maximum rate of photosynthesis, I <sub>k</sub> is the half saturation irradiance.....	13
<b>Figure 1.6</b> A typical growth rate vs. temperature response curve: A typical growth vs. temperature response curve; where T <sub>optimum</sub> is the temperature at which growth is maximal; CT <sub>min</sub> - minimum critical temperature and CT <sub>max</sub> : maximum critical temperature- below and above this temperature no algal growth is observed.....	14
<b>Figure 2.1:</b> Experimental ePBR setup: (a) square wave light, constant temperature regime (b) square wave light, sinusoidal temperature regime, SqLSiT, (c); sinusoidal light, constant temperature regime, SiLCT, (d) sinusoidal light, sinusoidal temperature regime, SiLSiT. Lines represent light intensity (solid line) and temperature (broken line). All irradiance cycles were 12 h: 12 h light: dark cycles of square-wave light (1240 μmol photons m <sup>-2</sup> s <sup>-1</sup> ), sinusoidal light 0 to 1920 μmol photons m <sup>-2</sup> s <sup>-1</sup> , with peak irradiance occurring at midday. Temperature cycles were as follows, constant 25 °C ± 0.5°C and sinusoidal temperature fluctuating between 20 - 30 °C with peak temperature occurring at dusk. ....	30
<b>Figure 2.2</b> Growth measurements: Cell abundance of <i>N. oculata</i> when cultivated in a ePBR under (a) square wave light, constant temperature, SqLCT (b) sinusoidal light, constant temperature regime, SiLCT, (c) square wave light, sinusoidal temperature regime, SqLSiT, and (d) sinusoidal light, sinusoidal temperature regime, SiLSiT. Symbols represent values for each replicate within each treatment; solid line represents the concatenated logistic fit (n=3) fitting using non-linear regression algorithm (OriginPRO 2015). The vertical coloured broken line represents the time at which, maximum oxygen concentration (blue), zero/minimal residue nitrate (magenta), zero/minimal residual orthophosphate (green) occurred. The dashed horizontal black line represents the predicted maximum cell number derived from the logistic fit.....	34

**Figure 2.3**  $pO_2$  profiles: *In situ* dissolved oxygen profiles of *N. oculata* when exposed to; (a) square wave light, constant temperature regime, SqLCT, (b) sinusoidal light, constant temperature regime, SiLCT (c) square wave light, constant temperature regime, SqLCT and (d) sinusoidal light, sinusoidal temperature regime, SiLSiT. Lines represent the average of 3 replicates (solid line)  $n=3$ , average  $\pm$  standard deviation (broken line) and a baseline (horizontal dotted line). The baseline value corresponds to the solubility of oxygen in seawater at 25 °C and 1 bar pressure. Dashed vertical lines correspond to the maximum oxygen concentration throughout growth..... 35

**Figure 2.4** Dissolved nutrient concentrations: Concentration of dissolved nitrate (a, c, e) and orthophosphate (b, d, f) throughout time in experiments carried out with *N. oculata* under square wave light, sinusoidal temperature regime, SqLSiT (a, b) sinusoidal light, constant temperature regime, SiLCT (c, d) and sinusoidal light, sinusoidal temperature regime, SiLSiT (e, f). The concentrations are expressed in  $\mu g L^{-1}$  each data point is represents and individual replicate, horizontal broken line represents 0  $\mu g L^{-1}$ . Vertical broken lines correspond to time at which predicted zero residual nutrient or minimal nitrate (magenta) and orthophosphate (green) nutrient amount occurred..... 37

**Figure 2.5** Dynamic oxygen and photophysiological response of *N. oculata*: Relative electron transport rate and *in situ*  $pO_2$  profiles of *N. oculata* when cultivated under different light and temperature regimes; (a, b) square wave light, sinusoidal temperature, SqLSiT; (c, d) sinusoidal light, constant temperature, SiLCT and (e, f) sinusoidal light, sinusoidal temperature regime, SiLSiT. Measurements were recorded at early exponential (a, c, e) and stationary phase (b, d, f). Solid diamonds and lines represent the average of 3 replicates relative electron transport rate and *in situ* dissolved oxygen profiles (blue line); error bars represent standard deviation ( $n=3$ ). The solid white area represents the light intensity at the surface of the culture. .... 39

**Figure 3.1** (a, b) Rapid light curves performed in the MC-PAM of replete cultures of *N. oculata* after exposure to 98  $\mu mol photons m^{-2} s^{-1}$  (PAR; white light) for 5 min at (a) 10 °C and (b) 40 °C, where closed diamonds represent triplicate samples ( $n=3$ ) and errors bars corresponding to  $\pm 1$  standard deviation. (c, d) Derived parameters of RLC curve fits at different temperature exposures where (c) maximum relative electron transport rate (circles) and (d) saturating irradiance (triangles)..... 58

**Figure 3.2** Relative electron transport rate (rETR) of *N. oculata* at different temperatures: rETR was determined using the multi-colour PAM (MC-PAM, Walz, Germany), samples were exposed to temperature for 5 min under 98  $\mu mol photons m^{-2} s^{-1}$  (PAR; white light) prior to performing a rapid light curve (10 s step). rETR was derived from the 54  $\mu mol photons m^{-2} s^{-1}$  light step. .... 59

**Figure 3.3** Relative electron transport rate (rETR) and maximum quantum yield of *N. oculata* after 24 hours at varying temperatures: (a) rETR corresponds to value at 2 seconds after induction of light performed on Imaging-PAM. (b) Maximum quantum yield was determined after dark adaption for 15 min. Symbols represent

the average of triplicates (n=3) with errors bars corresponding to  $\pm 1$  standard deviation. Square brackets cluster treatments where non-significant difference were found ( $p > 0.05$ ), whilst letters correspond to statistical difference between groups ( $p < 0.05$ ). ..... 60

**Figure 3.4** Physiological responses of *N. oculata* after 96 hours at varying temperatures: (a) specific growth rate (diamonds), (b) nitrate uptake rate (squares) and (c) orthophosphate uptake rate (circles) where symbols represent the average of triplicates (n=3) with errors corresponding to  $\pm 1$  standard deviation. Square brackets and letters represent groups of statistical different values ( $p < 0.05$ ). ..... 62

**Figure 3.5** Relative electron transport rate (rETR) and maximum quantum yield of *N. oculata* after 96 hours at varying temperatures: (a) rETR corresponds to value at 2 seconds after induction of light performed on Imaging-PAM. (b) Maximum quantum yield was determined after dark adaption for 15 min. Symbols represent the average of triplicates (n=3) with errors corresponding to  $\pm 1$  standard deviation. .... 63

**Figure 4.1** Schematic of nutrient supply experimental design. Solid diamonds represents treatments performed in this study with three replicates per treatment (n=3). Open diamonds represent treatments performed in Mayer et al. 2013 and open circles represent Rasdi and Qin 2015. Numbers represent treatment identification and asterisks indicate those samples chosen for total lipid quantification and fatty-acid methyl ester (FAME) analysis. Black diagonal line represents constant N:P ratios (24:1) with different magnitude of nutrient supply. Magenta and green broken lines represent samples cultivated under changing N:P, whilst maintaining consistent nitrogen and orthophosphate supply, respectively. The control treatment is traditional f/2 media (882  $\mu\text{M}$  nitrate and 36.2  $\mu\text{M}$  orthophosphate). ..... 79

**Figure 4.2:** Specific growth rates of *N. oculata* cultivated under a matrix of varying nitrate and orthophosphate supply. Bubbles size corresponds to the magnitude of growth rate; bigger bubbles indicate higher growth rates. Each bubble represents the average of triplicate samples (n=3). Similarities between treatments are denoted by same letters (one way ANOVA with post hoc Tukeys  $p > 0.05$ ), differences in treatments are denoted by different letters ( $p < 0.05$ ). ..... 83

**Figure 4.3:** Nutrient uptake dynamics of *N. oculata*; (a) Nitrate uptake (solid diamonds) and orthophosphate uptake (open circles) compared to the resulting cell specific growth rate. Solid and broken lines represent the linear regressions ( $y = mx + c$ ) for nitrate ( $m = 50.1$ ;  $R^2 = 0.71$ ) and orthophosphate uptake ( $m = 2.44$ ;  $R^2 = 0.20$ ) respectively. (b) Moles of N uptake per mole of P taken up in *N. oculata* cultivated under different N:P supply ratio. Closed circles represent the average of triplicate samples (n=3) with error bars corresponding to  $\pm 1$  standard deviation, a Michaelis-Menten model was fitted to the data (solid line;  $R^2 = 0.80$ ). ..... 84

**Figure 4.4** (a, b) Nutrient concentration of nitrate (solid diamonds), orthophosphate (solid circles) and maximum quantum yield,  $F_v/F_m$  (open squares) over a batch growth of *N. oculata* cultivated under (a) control (882  $\mu\text{M}$  N and 36.2  $\mu\text{M}$  P) and

(b) treatment 4 (176  $\mu\text{M}$  N and 7.24  $\mu\text{M}$  P) starting nutrient conditions. Vertical broken line represents the day in which nutrient depletion occurred, double headed arrow indicates time differential of nutrient depletion between the control and treatments 4. (c) Maximum quantum yield ( $F_V/F_M$ ) of *N. oculata* cultivated under a nutrient matrix measured on the day of harvest. Bubbles size corresponds to the magnitude  $F_V/F_M$  ( $n=3$ ) values are represented by scale-bar adjacent. Letters denote similarity to control (882  $\mu\text{M}$  N and 36.2  $\mu\text{M}$  P; one way ANOVA with post hoc Tukeys  $p > 0.05$ ), numbers represent the different treatment identification..... 86

**Figure 4.5** Biochemical analysis of *N. oculata* cultivated under a matrix of varying nitrate and orthophosphate supply. (a) Cellular lipid content ( $\text{pg cell}^{-1}$ ), bubble size corresponds to the cellular lipid content according to scale adjacent, where values represents the average of duplicate samples. Letters denoted significant difference in lipid content when compared with control (one way ANOVA with post hoc Tukeys  $p < 0.05$ ). (b) Eicosapentaenoic acid (EPA) percentage, bubble size corresponds to the magnitude of EPA % in scale adjacent. Each bubble represents the average of triplicate samples ( $n=3$ ). Similarity in treatments are denoted by same letters (one way ANOVA with post hoc Tukeys  $p > 0.05$ ), whilst different between treatments are denoted by different letters ( $p < 0.05$ )..... 90

**Figure 5.1** Schematic of oxygen concentration trace (blue line) used to calculate the gas transfer coefficient. Gas transfer rates were derived from equation 5.1 where the red solid line represents a typical fit,  $R^2 > 0.98$ . The vertical broken line represents the switching of gas types from  $\text{N}_2$  to ambient air and the horizontal broken line represents oxygen saturation..... 105

**Figure 5.2** (a) A typical dissolved oxygen trace of microalgae (solid blue line) cultivated under square wave light, white and gray background represents light on and light off respectively. Where the spike in the dissolved oxygen trace (a) were used to calculate (b) net photosynthesis and (c) respiration rates, both indicated by blue lines and gas transfer coefficient ( $k_L a$ ; b, c) indicated by red line..... 108

**Figure 5.3** Characterisation of gas transfer coefficient at different gas flow rates provided through different needle diameters of 0.21 mm (open diamond) and 0.34 mm (solid diamond). ..... 110

**Figure 5.4** Characterisation of gas transfer coefficients at different (a) temperature, (b) pH and (c) salinity using the ePBR set-up, each symbol represents the individual replicates. Broken line represents the gas transfer coefficient at 450  $\text{mL min}^{-1}$  at 26  $^{\circ}\text{C}$ , 0  $\text{g L}^{-1}$  and pH 5.93. .... 111

**Figure 5.5** (a) Growth of *N. oculata* under laboratory conditions (light intensity, white blocks), where temperature (red line), cell number (closed diamonds) were monitored over the growth cycle. Modelled rates of gas transfer (green line), photosynthesis (blue line), and respiration (black line) are shown during lag (a, d) and exponential (b,c) growth phases..... 114

**Figure 5.6** (a) Growth of *N. oculata* under simulated outdoor conditions obtained from raceway pond at UTS rooftop facility, where light intensity (white blocks),

temperature (red line) and cell number (closed diamonds) were monitored over the growth cycle. Modelled rates of gas transfer (green line), photosynthesis (blue line), and respiration (black line) are shown during lag (a, d) and exponential (b,c) growth phases. .... 115

**Figure 6.1:** Proposed method of bio-prospecting potential site for microalgae cultivation for biofuel production using the ePBR platform. .... 135

## List of Tables

<b>Table 1.1</b> Comparison of yield and land area requirement for common sources of biodiesel (modified from Chisti 2007). <sup>a</sup> Area required to produce 100% of Australia transport fuel (petrol and diesel), 30.6 billion litres (Australian Bureau of Statistics 2014). <sup>b</sup> 50% oil (by wt) in biomass. ....	4
<b>Table 1.2</b> Biomass, lipid content and lipid productivity of different microalgae cultivated under continuous light at 25 °C, modified from Rodolfi et al. 2009.....	12
<b>Table 2.1</b> Growth rate of <i>N. oculata</i> grown under square wave light, constant temperature (SqLCT) square wave light, sinusoidal temperature (SqLSiT); sinusoidal light, constant temperature (SiLCT) and sinusoidal light, sinusoidal temperature (SiLSiT). $\mu$ , growth rate expressed in $d^{-1}$ and final cell abundance expressed as $10^7$ cells per mL. Values are mean $\pm$ 1 SD (n=3) calculated using derived parameters from a non-linear logistic fit of individuals in each treatment. Asterisks correspond to the differences between treatments (one way ANOVA with post hoc Tukeys $p < 0.05$ ). ....	33
<b>Table 2.2</b> Nutrient uptake kinetics of <i>N. oculata</i> grown under square wave light, constant temperature (SqLCT) square wave light, sinusoidal temperature (SqLSiT); sinusoidal light, constant temperature (SiLCT) and sinusoidal light, sinusoidal temperature (SiLSiT). Nutrient uptake rates are expressed as $\mu g L^{-1} d^{-1}$ where values are mean $\pm$ 1 SD (n=3) calculated using derived parameters from a linear fit of individual replicates. Asterisk correspond to the differences between treatments (one way ANOVA with post hoc Tukeys $p < 0.05$ ). ....	36
<b>Table 4.1</b> Fatty acid composition of <i>N. oculata</i> cultivated under different nutrient concentrations: Fatty acids are expressed as a % of total fatty acid. Values are means of triplicate samples (n=3), $\pm 1$ standard deviation. ....	89

## Supplementary Figures

**Supplementary Figure 2.1** Dynamic oxygen and photophysiological response of *N. oculata*: Quantum yield of photosystem II and *in situ*  $pO_2$  profiles of *N. oculata* when cultivated under different light and temperature regimes; (a, b) square wave light, sinusoidal temperature, SqLSiT; (c, d) sinusoidal light, constant temperature, SiLCT and (e, f) sinusoidal light, sinusoidal temperature regime, SiLSiT. Measurements were recorded at early exponential (a, c, e) and stationary phase (b, d, f). Open diamonds and lines represent the average of 3 replicates relative electron transport rate and *in situ* dissolved oxygen profiles (blue line); error bars represent standard deviation (n=3). The solid white area represents the light intensity at the surface of the culture..... 50

**Supplementary Figure 3.1** Physiological responses of *N. oculata* after 24 hours at varying temperatures: (a) specific growth rate (diamonds), (b) nitrate uptake rate (squares) and (c) orthophosphate uptake rate (circles) where symbols represent the average of triplicates (n=3) with errors corresponding to  $\pm 1$  standard deviation. .... 72

**Supplementary Figure 3.2** Steady state light curve of *N. oculata*: rETR was calculated using the Imaging-PAM (Walz, Germany), samples were exposed to 5 min actinic light prior determination of relative electron transport rate. Symbols represent the average of triplicates (n=3) with errors corresponding to  $\pm 1$  standard deviation. Data from this analysis was used to determine the actinic light required for the induction curves..... 73

**Supplementary Figure 5.1** The environmental PBR set up used to determine gas transfer within the solution, the top two reservoirs allow for the water to be humidified, MFC are gas flow controllers and the solenoid switch allowed for the switching between nitrogen and air. .... 125

**Supplementary Figure 5.2** Dissolved oxygen trace ( $pO_2$ ) of *N. oculata* cultivated under (a) laboratory conditions (square- wave light) and (b) under simulated outdoor conditions. Spikes correspond to time points in which gas supply was switched off in order to calculate net photosynthesis/ dark respiration and gas transfer coefficients. .... 126

## Supplementary Tables

**Supplementary Table 2.1** Experimental photobioreactor set-up: All irradiance cycles were 12 h: 12 h light: dark cycles. .... **Error! Bookmark not defined.**

**Supplementary Table 4.1** Starting macronutrient concentrations ( $NO_3^-$  and  $PO_4^{3-}$ ): Asterisk (\*) represent samples chosen for lipid/ fatty acid methyl ester (FAME) analysis..... 97

## Abstract

The current global dependence on liquid fossil fuels is not sustainable and as a result, the development of alternative renewable liquid fuel sources is paramount for future economic, environmental and social security. The production of liquid biofuels from marine microalgae offers a solution, due to its carbon-neutral capacity (mitigating increasing anthropogenic carbon dioxide) and its minimal impact on existing food and freshwater resources. In order to satisfy global demand for liquid fuel, the cultivation of microalgae is required at commodity scales; however, major challenges exist in order to ensure production is economically and sustainably viable. The aim of this thesis was to assess some of the key environmental constraints of industrial scale cultivation of microalgae, including: exposure to complex abiotic conditions; effective delivery of nutrient inputs and harnessing algal physiology to improve the viability of microalgae cultivation for biofuel production. To accomplish these aims, the application of quantitative physiological techniques in conjunction with a novel photobioreactor platform (ePBR; Phenometrics®) enabled us to assess the biological response of a biofuel candidate algae strain, *Nannochloropsis oculata*, following exposure to different environmental conditions and nutrient input scenarios.

My thesis revealed complex responses of *N. oculata* to a variety of environmental conditions. The response to changing light and temperature environments was found to be influenced by the growth stage of the algal culture, whilst comparisons between productivity under laboratory versus simulated outdoor conditions showed sinusoidal light dominates the diel effect of temperature oscillations in determining final yields. Exposure of *N. oculata* to a range of temperature conditions emphasised the wide thermal envelope of growth and therefore, the suitability of this algae strain for use in biofuel production. Moreover, physiological algal traits were found to respond to the magnitude and duration of exposure to sub-optimal temperatures. Acclimation to nutrient conditions provide evidence of how natural cellular mechanisms can be harnessed to reduce the initial nutrient input, and how optimisation of nutrient delivery can be used to produce alternative products of interest. In my thesis, the suitability of the ePBR platform in conjunction with physiological methods such as *in vivo* chlorophyll fluorescence was used to examine the challenges of industrial cultivation. Several important avenues for future biofuel research are highlighted including: the better understanding of recovery of cultures from different magnitudes of environmental stress and harnessing the inherent acclimation process of microalgae to reduce system inputs will help to drive the future sustainability of the algal biofuels industry.